S1. Stratigraphy and new paleomagnetic data

Sediments in Block 2 above the 1.85 Ma Masavera Basalt are divided into two major stratigraphic units (see Fig. S1). Stratum A consists of a series of at least four separate ashfalls that conformably overlie the basalt. Stratum B deposits include horizontally extensive ashfalls, as well as a complex of deposits that filled pipes and the gullies that formed along collapsed pipes. The hominin remains in Block 2 were stratified within three subunits of Stratum B1, indicating a discrete sequence of accumulation. The first hominin bones were deposited in the lowest pipe-gully deposits of Stratum B1y, which overlies an erosional disconformity with Stratum A1. These are overlain by Stratum B1x, with numerous hominin bones that were gently scattered and quickly buried along the axis of the gully that formed along the W-E pipe axis. The superjacent gully fill (Stratum B1z), which contains one hominin remain, accumulated along a N-S axis.

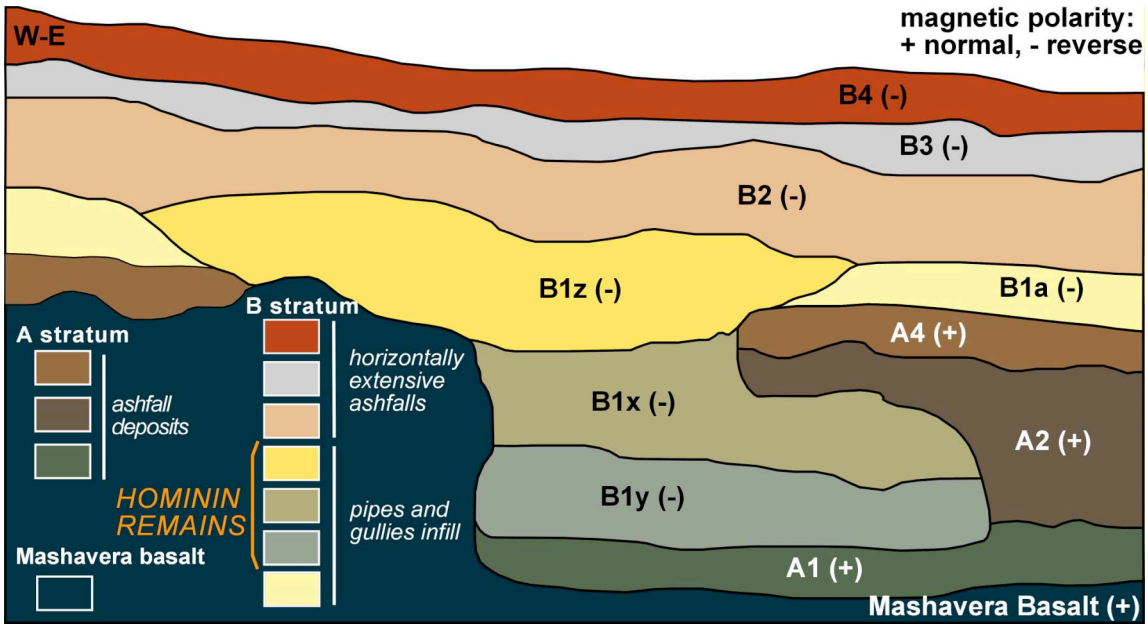

Supplementary Figure S1. Block 2 stratigraphic units, with indication of the units where hominin remains were found. Section is 10 m long, with ca. 1.8x vertical exaggeration.

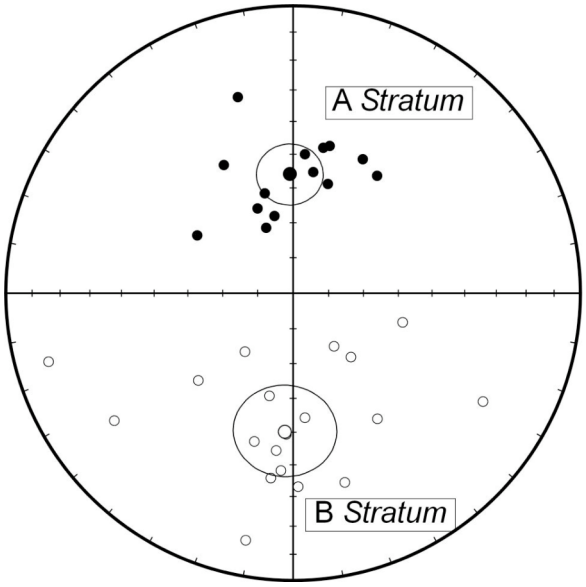

Mean directions:

	N	decl.	incl.	K	a95
Reverse (B *Stratum*)	19	183.4	-50.0	6.9	13.8
Normal (A *Stratum*)	14	358.4	55.9	20.4	9.0

Sample directions:

A samples	declination	inclination
A1B	27.5º	46.3º
A1C	346.5º	67.5º
A1D	35.6º	48.3º
A21A	9.4º	54.9º
A21B	14.0º	46.1º
A22A	11.7º	47.1º
A4C	301.1º	58.0º
A4A	4.9º	49.8º
A4B	337.2º	63.8º
ASA	17.6º	57.2º
ASB	337.7º	70.0º
ASG	331.6º	48.0º
ASH	344.2º	60.4º
ASI	344.3º	29.8º

B samples	declination	incl.
B1YB	227.3º	-53.0º
B1YBbis	219.5º	-68.5º
B1YC	146.1º	-46.2º
B1AA	190.9º	-13.5º
B1AB	234.5º	-24.6º
B1AC	254.3º	-12.6
B1ZA	104.9º	-57.6º
B1ZB	194.6º	-45.7
BY44A	174.5º	-54.1º
BY44	164.7º	-32.3º
PB2A	183.9º	-38.1º
PB2E	193.0º	-59.9º
PB2C	186.1º	-44.2º
PB2D	178.5º	-33.1º
BMA	186.9º	-35.4º
BMB	137.8º	-65.5º
BMC	182.7º	-49.3º
BME	142.5º	-71.0º
BMF	119.7º	-24.9º

Supplementary Figure S2. Individual characteristic remnant magnetization values. Left: stereographic plot (open and filled dots belong to the southern and northern hemisphere, respectively). Tables: values per sample. Note that all samples from A stratum display northern declinations and positive inclinations. Conversely, B stratum samples are southwards directed and show negative inclinations. Thus, A and B stratum display normal and reverse polarities, respectively. N=number of samples, decl. = declination, incl.= inclination, K and a95 = Fisher statistic values.

The upper part of the Stratum A deposits exhibit weak pedogenic features, and the contact between A and B is a minor erosional disconformity. The first paleomagnetic analyses of Block 2 deposits (see Figs. S1 and S2) revealed that all of the Stratum A deposits in Block 2 exhibit normal geomagnetic polarity, while all of the Stratum B1y to B2 deposits exhibit reversed polarity (adjacent to Block 2, B3 and B4 also display reversed polarity). These new data are fully concordant with the initial stratigraphic and paleomagnetic studies of Block 1[2]. Despite this change of polarity, the presence of the same rodent species of the genera *Cricetulus* and *Parameriones* in both A and B1y strata confirms that there is not a significant chronological gap between them.

S2. Fauna and biostratigraphy

Apart from the hominin record, the Dmanisi fossil vertebrate assemblage (Table S1) comprises so far remains of 44 taxa of amphibians (1), reptiles (3), birds (3) and mammals (37). Most of the micromammal species from Dmanisi correspond to typical Late Pliocene forms, such as *Mimomys pliocaenicus* and *Tcharinomys tornensis*, two characteristic voles of the Villanyian small mammal age (equivalent to the Tiglian). The large mammal association of Dmanisi reflects the time span of transition from Middle to Late Villafranchian in character. Several of the recorded elements are well known from Late Pliocene contexts in western Asia and Europe: *Pliocrocuta perrieri*, *Mammuthus meridionalis* (typical form), *Eucladoceros* aff. *tegulensis*, *Palaeotragus*, *Gallogoral meneghinii sickenbergii*. More modern forms are represented by, e.g., *Cervus* (*Pseudodama*) cf. *nestii*, *Bison* (*Eobison*) *georgicus*, and *Pontoceros* sp. The absence of raccoon dog (*Nyctereutes*) within the huge amount of recorded fossils could support the idea of a slightly younger than Middle Villafranchian mammal age.

Supplementary Table S1. Faunal list of the Dmanisi site

Class	Order	Family	Genus	Species
Amphibia				
	Anura	Bufonidae	*Bufo*	*viridis*
Reptilia				
	Testudinata	*Testudinidae*	*Testudo*	*graeca*
	Squamata	*Lacertidae*	*Lacerta*	*ex. gr. viridis*
		Colubridae	*cf. Elaphe*	*quatuorlineata*
Aves				
	Struthioniformes	Struthionidae	*Struthio*	*dmanisensis*
	Galliformes	Gallidae	*Gallus*	*dmanisiensis*
	Strigiformes	Strigidae	*Strix*	*gigas*
Mammalia				
	Insectivora	Soricidae	*Sorex*	sp.
	Lagomorpha	Ochotonidae	cf. *Ochotona*	*lagreli*
		Leporidae	cf. *Hypolagus*	*brachygnathus*
	Rodentia	Muridae	*Apodemus*	aff. *atavus*
		Cricetidae	*Cricetulus*	sp.
		Arvicolidae	*Tcharinomys*	*tornensis*
			Mimomys	*pliocaenicus*
		Gerbillidae	*Paramerione*s	aff. *obeidiensis*
		Hystricidae	*Hystrix*	*refossa*
	Carnivora	Canidae	*Canis*	*etruscus*
			Vulpes	*alopecoides*
		Ursidae	*Ursus*	*etruscus*
			Ursus	sp.
		Mustelidae	*Martes*	sp.
			Meles	sp.
		Hyaenidae	*Pliocrocuta*	*perrieri*
			Pachycrocuta	sp.
		Felidae	*Lynx*	*issiodorensis*
			Acinonyx	*pardinensis*
			Panthera	*onca* ssp.(=
			Megantereon	*megantereon*
			Homotherium	*crenatidens*
	Proboscidea	Elephantidae	*Mammuthus*	*meridionalis*
	Perissodactyla	Equidae	*Equus*	*stenonis*
			Equus	aff. *altidens*
		Rhinocerotidae	*Stephanorhinus*	*etruscus*
	Artiodactyla	Cervidae	*Cervus*	cf. *nestii*
			Cervus	*abesalomi*
			Eucladoceros	aff. *tegulensis* (= *senezensis*)
		Giraffidae	*Palaeotragus*	sp.
		Bovidae	*Bison (Eobison)*	*georgicus*
			Gallogoral	*meneghinii sickenbergii*
			Capra	*dalii*
			Soergelia	cf. *minor*
			Ovibovini indet.	
			Pontoceros	sp.
			Antilopini indet.	

S3. Palaeozoogeography

According to Fortelius *et al.*[51] the genus-level faunal resemblance index is calculated using both Simspon's[52] and Dice's[53] faunal resemblance indexes. The Dice index is the one most highly recommended by Archer and Maples[54] and Maples and Archer[55] and is calculated as 2A / (2A + B + C), where A is the number of taxa present in both faunas, B is the number of taxa present in fauna 1, but absent in fauna 2, and C is the number of taxa present in fauna 2 but absent in fauna 1. Simpson's faunal resemblance index (calculated as A / (A + E), where E is the smaller of B or C has a long tradition of use in studies of similarity of fossil mammals[56-58] and is coupled with Dice index in Figure S3**.**

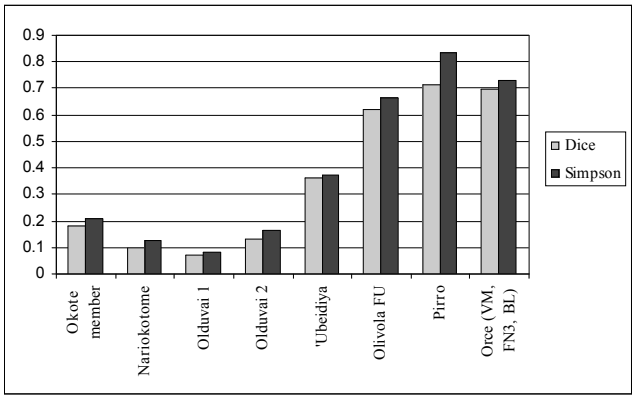

Supplementary Figure S3. Genus-level faunal comparison of Dmanisi large mammals assemblage with various Plio-Pleistocene assemblages from Africa, the Near East and Europe showing that Dmanisi has resemblance values with European Late Villafranchian mammal faunas. Data source updated by one of us (LR) from Turner *et al.*,[59] and from the Neogene of the Old World Database of Fossil Mammals (NOW public release 030717, www.helsinki.fi/science/now/).

The highest similarity values of the Dmanisi faunal assemblage are with W-European "Late Villafranchian" assemblages, while the "African" mammal faunas show very low GFRI values. Similarities between Dmanisi and African assemblages are mainly due to the co-occurrence of common carnivore genera (e.g. *Homotherium*, *Megantereon*, *Panthera*) or, among herbivores, widespread genera like *Equus*.

S4. Palaeoecology

The combination of topographic and vertebrate palaeontological information allows to infer a differentiated landscape pattern. Over a distance of a few kilometres, the landscape character changed from a flat and fairly wet river valley with gallery forests (indicated especially by the frequently recorded *Eucladoceros* and the elaphine deer *Cervus abesalomi*) to flanking slopes with shrub vegetation of varying densities, turning into dry meadows in the southerly exposed areas with more intense insolation. Extended tree savannah to open grasslands characterised the higher ground out of the valley. In addition to savannahs, semidesert-like rocky terrains existed on the lava outcrops in the vicinity of the site. *Testudo graeca* and *Hystrix refossa* indicate temperate climatic parameters.

Supplementary Table S2. Ecological characteristics of selected taxa and Dmanisi site inferred landscape

dense to open forests and shrub landscapes	tree savannah and open grasslands	rocky, semi-arid terrains
Eucladoceros aff. *tegulensis* (= *E*. aff.	cf. *Ochotona lagreli*	*Capra dalii*
		Gallogoral meneghinii
Cervus (Pseudodama) cf. *nestii*	*Parameriones* aff.	
Meles sp.		
Sorex sp.	Antilopini indet.	
Apodemus aff. *atavus*	*Equus* aff. *altidens*	
Bison (Eobison) georgicus (most probably)		
Strix gigas (most probably)		
Stephanorhinus etruscus (partly)	*Stephanorhinus etruscus*	
Mammuthus meridionalis (partly)	*Mammuthus meridionalis*	

S5. Taphonomy

The Dmanisi large mammal assemblage is well preserved with little subaerial weathering. 72% of specimens are in weathering stage 0, 21% in stage 1, and 5% in stage 2[60, 61]. This signal, along with the presence of several articulated body segments, indicates rapid burial after death. Post-burial surface damage such as fungal/root etching is common.

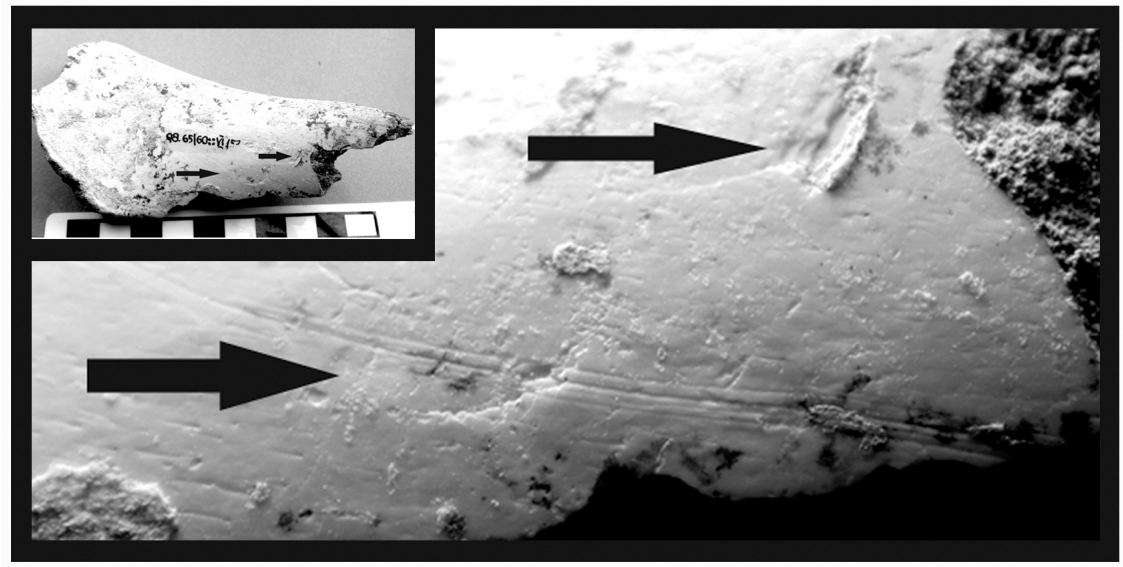

Supplementary Figure S4. Shaft fragment of a mammal size class 3 humerus with stone tool cut mark found under calcrete (lower arrow; size classes after[62]). A pit from either a hammerstone, or carnivore (upper arrow). The lack of striations in the pit suggests it is a carnivore tooth mark, which would appear to document that a carnivore broke the bone open for marrow after hominins consumed the meat. Scale bar is in cm.

One third of plotted bone specimens are unbroken. Of breaks, 50% have curved morphology and acute angles, and 21% are intermediate in form, indicating breakage while the bone was still fresh, rather than after fossilization such as breaking due to transport or crushing by sediments[63]. In addition, the absence of trample marks or other evidence of transport, suggests that most of the bones were broken during consumption.

Stone tool marks are rare, observable on less than 1% of the assemblage (see Figs. S4 and S5), but their presence does indicate that the hominins were eating meat, and with the presence of the multiple stone tools and manuports, they indicate that hominins were living in the direct vicinity of the site. The presence of cutmarks on a few mid-shaft upper limb bones (humerus/femur) indicates the hominins were filleting meat, and that a large carnivore such as a felid or hyaenid did not consume the meat first, and therefore that hominins had early access to carcasses. Carnivore tooth marks are present in higher frequencies in the assemblage than tool marks, and are on about 8-9% of the bones; hyena and other carnivore coprolites are also present. The small amount of carnivore damage is less than expected if bone-crushing hyenas accumulated the hominin bones. [64, 65]. Like the mammals, most of the hominin fossils exhibit no subaerial weathering and very little other damage. The presence of skeletal elements that almost never survive carnivore consumption, such as the 3 clavicles, first ribs, and patella, suggests that the hominins were not consumed by large carnivores[66, 67].

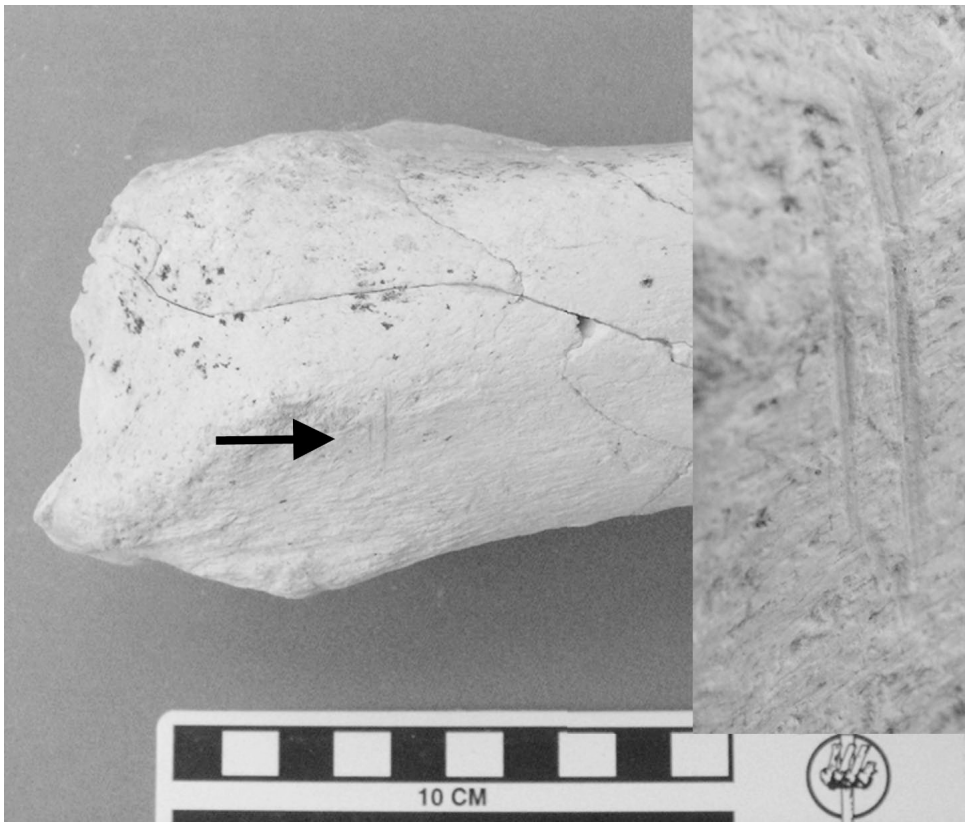

Supplementary Figure S5. *Bison* (*Eobison*) *georgicus* distal radius with a striated cut mark (1x14.9 mm) running perpendicular to the long axis.

S6. Dmanisi hominin postcranial material of subadult individual

Supplementary Table S3. Assessment of developmental stage of subadult cranial and postcranial hominin elements

Dmanisi palaeontological nr.	bone	developmental stage markers	modern human developmental age (y)[1]
D2700	cranium	third molar root 30%; spheno-occipital synchondrosis unfused	<15
D2735	mandible	agenesis of left third molar; germ of right third molar is missing	-
D2724	clavicle		-
D2715 and D2680	humerus	two out of seven secondary points of ossification are unfused: medial epicondyle and proximal epiphyses	females: 13-17 males: 14-20
D2721; D2673; D2713; D2627	vertebrae	no annular epiphyseal fusion	females: 18 males: 18.9
D2679; D2670; D3480	phalanges	epiphyseal fusion	females: 11-13 males: 14-16
D2671	metatarsal I	epiphyseal fusion incomplete	females: 13-15 males: 16-18
D2669	metatarsal IV	epiphyseal fusion	females: 11-13 males: 14-16

[1] comparative data from Scheuer & Black (ref. 68)

S7. Comparative morphometric data

Linear measurements were taken using metric callipers; maximum lengths of humerus, tibia and femur were measured using an osteometric board. Circumferences were measured with a sliding osteometric ruler. All measurements were taken to the nearest millimetre. Angular measurements were obtained from digital images using ImageJ version 1.32J (National Institutes of Health, http://isb.info.nif.gov/ij/).

The extant comparative series includes adult and subadult samples of modern *Homo sapiens*, *Pan troglodytes*, *Gorilla gorilla*, and *Pongo pygmaeus*. Samples are from the Royal Museum of Central Africa (Tervuren, Belgium), the National Museum of Natural History, Paris, and the Anthropological Institute of the University of Zurich. The modern human samples are from the archaeological sites of Karagunduz (Ankara University, Turkey) and the Necropoles of Isola Sacra, Taforalt and Afalou (Institut de Paléontologie Humaine, National Museum of Natural History, Paris).

Linear osteometric dimensions follow the definitions of Martin and Saller[69]. In the scapual, glenoid orientation relative to the spine corresponds to the angle between the base of the spine and the long axis of the glenoid cavity[70]. The glenocoracoid angle expresses the orientation of the distal extremity of the coracoid process in relation to the main axis of the glenoid cavity. In the humerus, the position of the lateral condyle is measured by the ratio between the height of the capitulum and the height of the lateral epicondyle. Because humeral heads are not preserved in the Dmanisi sample, torsion was measured on the diaphyses. Using a Microscribe 3DX digitizer, four landmarks were determined on the proximal and distal extremes of the diaphysis: on the proximal end, the most salient point in the middle of the greater tubercle (A) and the most posterior point on the anatomical neck (B); on the distal end, the most salient points on the lateral (C) and medial (D) epicondyles. Torsion was defined as the angle between vectors (A-B) and (C-D). Vertebral zygapophyseal orientation was measured, in posterior view, as the angle between the midsagittal line and a line parallel to the prezygapophyseal articular surface[71]. In C2, the anterior angle of the superior articular process was measured in anterior view between lines parallel to the left and right articular surfaces.

Supplementary Table S4. Univariate comparison of postcranial elements[1].

Measurements[2]	australopiths[3]	earliest *Homo*[3]	Dmanisi	KNM-WT15000	*Homo sapiens*[3]	*Pan troglodytes*[3]	*Gorilla gorilla*[3]
Scapula							
Olecranon direction relative to midaxillary border (M17)	116.0 – 115.0 2 [4]	-	129.0	127.0	141.7±4.7 133.8 – 154.0 30	117.7±5.8 107.7 – 128.9 30	121.8±5.3 113.3 – 132.3 29
Coracoid process width to length ratio	-	-	41.2	-	33.1±2.9 28.4 – 38.6 30	38.15±3.9 31.5 – 48.9 30	44.8±6.2 32.1 – 57.2 29
Coracoid process width			13.5		15.5±1.7 11.0 – 19.0 30	15.9±1.7 13.1 – 19.2 30	28.2±5.8 19.2 – 42.1 30
Coracoid process length			32.8		49.9±4.8 37.0 – 54.9 30	41.9±2.9 37.5 – 49.9 30	63.1±9.3 48.0 – 83.3 30
Spine process breadth to width ratio	-	-	54.0	57.7	55.2 ±5.5 42.5 – 65.4 30	16.2±4.1 10.9 – 27.9 30	16.6±3.2 10.6 – 23.0 29
Length of spine			26.3	39.53	49.3±5.9 36.9 – 59.2 30	45.8±4.9 37.2 – 54.8 30	67.3±12.2 48.2- 83.1 29
Width of spine			14.2	22.8	27.0±3.0 22.0 – 32.8 30	7.31±1.5 5.0 – 12.1 30	11.3±2.7 6.8 – 17.4 30
Glenoid orientation relative to the spine	-	-	81.0	75.0	89.4 ±6.5 79.9 – 102.9 30	55.8±7.2 41.0 – 67 30	59.0±9.6 40.0 – 78.5 29
Glenocoracoid angle			55.0	59.5	82.5±7.6 60.0 – 94.5 29	48.78±7.1 31.0 – 64.5 30	45.1±12.0 20.0 – 68.0 38
Clavicle							
Length	-	149.4[5]	137.03 – 135.6 2		137.0±10.9 113.0 - 159.0 50	118.0±11.5 97.4 – 140.2 33	148.5±15.3 126.9 – 161.2 27
			123.2	*130.5*	*127.2±7.4* *113.6 – 139.0* *13*	*106.09±8.3* *93.5 – 117.6* *8*	*148.6±15.3* *126.9- 181.2* *8*
Shape at midshaft (a-p/s-i diameters)	-	79.0[5]	79.3 – 67.2 2		76.7±9.4 57.9 – 97.3 50	70.75±10.3 46.6-89.7 33	71.0±10.4 54.9 – 100 27
			80.6	*53.8*	*80.5±11.3* *60.9 – 100* *13*	*80.2±12.1* *61.1 – 98.1* *8*	*73.4±3.6* *66.6 – 79.3* *8*
Shape at conoid tubercle (a-p/s-i diameters)	-	78.2[5]	80.6 – 80.2		60.7±11.3 40.9 – 92.3 50	42.1±4.7 33.1 – 52.6 33	52.6±5.5 38.9 – 62.6 27
			63.0	*85.1*	*62.9±9.2* *44.4 – 77.3* *13*	*39.6±4.0* *32.8 – 44.3* *8*	*52.5±4.9* *45.1 – 60.3* *8*
Humerus							
Length (M1)	235.0 – 226 2[6]	-	295.0		304.0±16.6 263.0 -341.0 38	290.3±21.6 259.0 – 326.0 33	404.8±44.7 342.0 – 466.0 31
			282.2	*319.0*	*298.2±22.7* *255.0 – 334.0* *27*	*272.7±21.0* *234.0 – 296.0* *8*	*403.6±40.3* *367.5 – 441.0* *6*
Torsion (M18)	122.7 111.0 – 130.0 4[7]	-	110.0		155.3±9.8 134.9 – 180.0 38	147.9±8.0 128.7 – 164.4 31	149.6±6.0 137.5 – 159.6 31
			104.0	*146.0*	*150.8±5.9* *138.2- 160.7* *23*	*147.7±6.1* *136.6 – 155.1* *8*	*152.6±4.7* *144.5 – 158.8* *6*
Lateral condyle position	91.5±4.7 85.0 – 98.4 7[8]	89.2[9]	85.8		112.5±11.1 92.1 – 132.3 38	76.9±6.5 62.0 – 86.9 29	73.1±4.7 63.1 – 81.6 27

Measurements[2]	australopiths[3]	earliest *Homo*[3]	Dmanisi	KNM-WT15000	*Homo sapiens*[3]	*Pan troglodytes*[3]	*Gorilla gorilla*[3]
			76.0		*109.0±15.3* *78.1 – 131.3* *21*	*103.7±14.6* *78.0 – 120.0* *8*	*66.6±6.5* *61.0 - 77.7* *6*
Vertebrae							
C2 anterior angle of sup. art. proc.	*107.0 – 120.0* *2*[10]	-	*111.0*	-	*136.0±6.4* *129.1 – 147.2* *10*	*110.5±3.2* *106.4 – 115.1* *6*	*112.3±1.4* *110.8 – 114.3* *6*
C2 canal shape (M11/M10)	-	-	*115.27*	-	*121.4±9.9* *131.9 – 108.7* *10*	*90.9 ±4.5* *85.1 – 97.7* *6*	*78.0± 6.4* *69.8 – 85.9* *6*
C3 canal shape (M11/M10)	-	-	*150.0*	-	*130.5±14.4* *113.7- 160.0* *10*	*83.1±7.3* *73.7 – 93.0* *6*	*98.3±5.0* *90.7 – 105.4* *6*
Zygapophyseal joint angles C2/C3			*62.5*		*73.4±6.8* *64.60 – 83.6* *10*	*49.6±3.6* *46.3 – 54.8* *6*	*59.6±5.9* *52.3 – 69.0* *6*
Th3 canal shape (M11/M10)	-	-	*114.8*	*110.2*	*109.5±7.8* *100.7 – 115.5* *10*	*94.4±5.5* *86.7 – 96.4* *6*	*90.8±3.5* *86.7 – 96.4* *6*
Th10 canal shape (M11/M10)	-	-	*100.8*	*100.4*	*104.2±7.6* *100.6 – 107.8* *10*	*87.9±9.4* *75.2 – 99.1* *6*	*88.4± 8.6* *76.2 – 98.6* *6*
Th10 centrum area (M4*M7)			*692.2*		*759.2±113.9* *601.1 – 958.6* *10*	*460.9±85.3* *308.0 – 565.8* *6*	*665.0±186.7* *444.6 – 964.7* *6*
Th10 centrum shape (M4/M7)			*111.6*		*136.0±13.6* *113.1 – 153.1* *10*	*121.5±9.3* *106.9 – 131.7* *6*	*126.6±10.8* *114.6 – 150.0* *6*
Th10 zygapophyseal joint angle Th10/Th11			*107.6*		*106.4±4.6* *100.0 – 113.4* *10*	*109.1±4.1* *105.3 – 115.4* *6*	*114.6±3.6* *111.0 – 119.7* *6*
L1 canal shape (M11/M10)	-	-	*80.8*	-	*87.7±8.0* *74.8 – 101.0* *10*	*115.2±6.8* *105.6 – 126.3* *6*	*120.1±11.8* *104.6 – 133.3* *6*
L1 centrum area (M4*M7)	-	-	*777.8*	*803.4*	*940.6±165.9* *706.3 – 1288.9* *10*	*772.4± 95.9* *575.4 – 836.9* *6*	*878.0± 284.8* *610.0 – 1334.0* *6*
Th10 centrum shape (M7/M4)			*114.2*		*148.8±9.0* *134.5 – 169.1* *10*	*133.5±9.2* *120.0 – 143.4* *6*	*153.7±9.7* *140.2 – 166.7* *6*
L1 zygapophyseal joint angle L1/L2	29.0[11]		*45.6*		*31.6 ±5.3* *24.5 – 40.0* *10*	*34.4±4.8* *26.8 – 38.9* *6*	*72.5±9.3* *61.6 – 84.2* *6*
Femur							
Length (M1)	280.0[12]	401.0 – 396.0 2[13]	386.0	432.0	381.9±22.9 337.0 - 434.0 22	290.2±15.9 252 - 318 30	350.1±40.8 294.0 - 423 30
Medial to lateral condylar breadth (M21c/M21e)	108.4 100.0 – 125.0[14]	87.7 – 107.9 2[13]	103.9	-	121.6±12.2 103.2 – 143.3 30	121.5±16.2 104.0 -148.6 30	139.8±14.1 119.4 – 171.8 26
Neck index (M16/M15)	69.8 64.6 – 78.2 6[15]	88.9 – 95.3 2 [13]	66.2	78.5	80.4±6.3 63.4 – 93.1 30	83.3±4.6 72.1 – 90.1 30	76.7±5.1 65.8 – 88.9 30
Bicondylar angle (M30)	77.0 75.0 – 81.0 7[16]	77.0 -80.0 2[13]	81.5	80.0	80.3±2.8 76.0 – 88.0 30	89.3±2.9 85.0-96.2 30	89.5±2.2 85.0 - 95.0 30
Tibia							
Length (M1a)	-	-	306.0	380.0	318.9±20.5 290.0 - 374.0 22	242.2±14.3 207.0 – 266.0 30	281.5±29.7 241.0 – 334.0 30
Midshaft index (M9/M8)	-	70.1 63.9 - 81.5 3[17]	66.6	83.3	60.9±6.0 48.1 – 68.2 26	67.9±6.7 56.6 – 80.5 30	76.5±7.0 62.5 – 91.4 30
Angle of torsion (M14)	-	-	21.9		20.1±7.1 7.8 – 33.8 26	33.8±6.8 21.5 – 45.8 30	27.4±5.4 20.2 – 39.3 30

Measurements[2]	australopiths[3]	earliest *Homo*[3]	Dmanisi	KNM-WT15000	*Homo sapiens*[3]	*Pan troglodytes*[3]	*Gorilla gorilla*[3]
Angle of inclination (M13)	-	-	82.0		97.2±4.6 89.1 – 111.7 26	75.1±4.5 65.4 – 82.7 30	82.5±4.4 72.3 – 90 30
Talus							
Neck angle (M16)	32.3 26.9 – 37.0 6[18]	33.5[19]	26.	-	19.4±4.9 12.0 – 31.0 30	34.4±3.9 25.4 – 42.5 30	32.4±3.8 23.5 – 36.7 30
Metatarsals							
Angle of torsion of metatarsal I (M11)	-	-	*3 – 15* *2*	-	13.9±7.1 3.5 – 32.0 30	40.1±17.4 24.2 – 54.5 28	47.5±10.8 31.4 – 68.9 30
Index of shaft of metatarsal I (M3/M4)	105.8 102.9 – 111.6 3[20]	-	*102.6 – 106.8* *2*	-	95.2±8.6 81.9 – 115.6 30	90.8±6.8 75.8 – 102.0 28	93.5±10.6 76.9 – 114.9 30
Angle of torsion of metatarsal III (M11)	-	23.6[19]	26.9 – 21.7 2	-	17.5±6.1 5.0 – 30.0 30	13.3 ±3.0 8.6 – 19.5 27	12.6±3.4 4.7 – 19.7 30
Index of shaft of metatarsal III (M3/M4)	-	63.1 – 75.3 2[21]	69-4 – 87.3 2	-	91.1±9.5 72.8 -107.0 30	74.1±6.1 64.5 - 86.6 27	74.1±8.4 53.7 – 90.9 30
Angle of torsion of metatarsal IV (M11)	-	28.2[19]	27.8 – 29.0 2	-	18.7±6.7 1.5 – 30.0 30	8.9±3.0 3.5 – 14.9 24	9.9±3.8 3.6 – 18.9 30
Index of shaft of metatarsal IV (M3/M4)	-	80.7[19]	68.1 – 75.5	-	99.6±11.4 78.3 – 122.1 30	86.5±7.2 73.9 -106.6 30	75.1±8.7 57.6 – 100.3 30
Angle of torsion of metatarsal V (M11)	-	-	6.7	-	11.7±6.4 2.8 – 27.8 30	13.2±3.8 5.8 – 23.4 30	15.9±5.6 5.9 – 26.4 30
Index of shaft of metatarsal V (M3/M4)	102.73[22]	127.80[19]	135.4	-	136.9±11.0 116.1 – 156.7 30	114.2±12.4 90.1 – 131.7 30	93.9±16.7 68.9 – 131.9 30

[1]Linear measurements are in mm, angular measurements are in degrees; [2]Measurement codes according to Martin (ref. 69); [3]Measurements are represented by mean ± std.dev., range, and sample size; data for subadults are in italics; [4]Sts7, AL288-1; [5]OH48; [6]AL288-1, Bou-VP-12/1; [7]AL288-1, ER739, Sts7, Omo119; [8]AL288-1, AL137-48, AL322-1, KP271, ER739, TM1517, Stw431c; [9]ER1504; [10]AL333-101, SK-854; [11]Sts-14f; [12]AL288-1; [13]ER1481, ER1472; [14]AL129, AL333-4, Sts34, TM1513; [15]AL288-1, AL333-3, AL333-95, F.SK26, SK82, ER1505; [16]AL288-1, AL129-1a, AL333-4, AL333w-56, Sts34, TM1513, ER993; [17]HO35a, KNM-ER813a, KNM-ER741; [18]AL288-1, TM1517, ER1476a, ER813, ER1464, Stw573; [19]OH8; [20]SK1813, SKX5017, Stw562; [21]KNM-ER1823, OH8; [22]AL333-13.

S8. Estimates of stature, body mass and encephalization quotient (EQ)

Limb proportions of the Dmanisi hominins, measured by femoro-tibial and humero-femoral ratios are similar to those of modern humans. It is thus sensible to use modern human prediction equations to estimate body mass (Table S5) and stature (Table S6) of the Dmanisi hominins.

Body mass estimates were calculated using the equations for femur, humerus, tibia, and metatarsal I[72]. The inferred body mass of the large adult individual is between 47.6 kg and 50.0 kg. The body mass of the small adult individual, calculated from the first metatarsal (D2671)[72] is 40.2 kg. Based on humeral and femoral dimensions, the body mass of the subadult is between 40.0 kg and 42.5 kg.

Stature estimates for the subadult Dmanisi individual were obtained with prediction equations for juvenile samples[42]; estimates based on humeral length (D2680) yield a value between 144.9 cm and 161.4 cm. Stature estimates for the large adult individual were obtained from humeral, femoral, and tibial dimensions[73, 74], yielding a range of 146.6 cm – 166.2 cm. Stature estimates based on the length of the first metatarsal (D3442)[75] yield a value of 143.0 cm.

Brain mass was estimated from endocranial volumes using the formula provided by Martin[76]. The encephalization quotient was evaluated according to the formula provided by Martin[77], using 95% confidence ranges for body mass estimates of each individual (Table S7).

Supplementary Table S5. Estimation of body mass in Dmanisi individuals

	specimen	Dimension1 (mm)	Dimension2 (mm)	Estimated body mass (kg)	95% confidence interval (kg)	95% confidence range (kg)	Comparative modern human sample	Data source (ref.#)
Subadult								
Elbow	D2680	38.0[1]	14.4[2]	38.5	1.3	37.2 - 39.8	female	41
		38.0[1]	14.4[2]	38.5	1.3	37.2 - 39.8	male	41
Femoral shaft	D3160	21.4[3]	25.3[4]	44.0	1.2	42.8 - 45.2	female	41
		21.4[3]	25.3[4]	44.0	1.2	42.8 - 45.2	male	41
Average				**41.2**		**40.0 - 42.5**		
Adult (large)								
Elbow	D4507	40.2[1]	17.9[2]	48.9	1.3	47.6 - 50.2	female	41
		40.2[1]	17.9[2]	48.9	1.3	47.6 - 50.2	male	41
Femoral head	D4167	40.0[5]		49.6	1.2	48.4 - 50.8	female	41
		40.0[5]		49.6	1.2	48.4 - 50.8	male	41
Proximal tibia	D3901	40.5[6]	67.3[7]	48.1	1.1	46.9 - 49.2	female	41
		40.5[6]	67.3[7]	48.1	1.1	46.9 - 49.2	male	41
Distal tibia	D3901	27.1[8]	26.0[9]	48.6	1.2	47.4 - 49.8	female	41
		27.1[8]	26.0[9]	48.6	1.2	47.4 - 49.8	male	41
Average				**48.8**		**47.6 - 50.0**		
Adult (small)								
MT I base	D3442	22.3[10]	16.4[11]	39.7			composite	72
MT I head	D3442	15.7[12]	16.3[13]	40.7			composite	72
Average				**40.2**				

[1]articular width of the distal humerus; [2]capitular height; [3,4]antero-posterior and transversal diameters of the femoral shaft, taken just inferior to the lesser trochanter; [5]maximum supero-inferior diameter of the femoral head; [6,7]antero-posterior and transversal diameter respectively of the proximal tibia; [8,9]antero-posterior and transversal diameter respectively of the talar facet on the distal tibia; [10,11]medio-lateral and dorsoplantar diameter respectively of the base of metatarsal I; [12,13]medio-lateral and dorsoplantar diameter respectively of the head of metatarsal.

Supplementary Table S6. Estimation of stature in Dmanisi individuals

		Length (cm)	Stature estimate (cm)	95% confidence interval (cm)	95% confidence range (cm)	Comparative sample	data source (ref. #)
Subadult							
Humerus	D2680	28.2	152.7	8.6	144.1 - 161.4	subadult (12y)	42
		28.2	153.5	7.9	145.6 - 161.5	subadult (13y)	42
Average			**153.1**		**144.9 - 161.4**		
Adult (large)							
Humerus	D4507	29.5	161.5	11.1	150.4 - 172.5	Caucasian (m)	73
		29.5	159.6	9.6	149.9 - 169.2	Caucasian (f)	73
		29.5	159.6	10.4	149.2 - 169.9	African (m)	73
		29.5	158.0	9.2	148.8 - 167.3	African (f)	73
		29.5	145.7			African (m)	78
		29.5	143.0			African (f)	78
Femur	D4167	38.6	154.5	9.2	145.3 - 163.7	Caucasian (m)	73
		38.6	152.6	8.6	144.1 - 161.2	Caucasian (f)	73
		38.6	155.7	11.2	144.4 - 166.9	African (m)	73
		38.6	151.2	8.3	142.8 - 159.5	African (f)	73
		38.6	138.5			African (m)	78
		38.6	134.3			African (f)	78
Tibia	D3901	30.0	157.2	10.0	147.2 - 167.3	Caucasian (m)	73
		30.0	153.6	10.3	143.3 - 163.9	African (m)	73
		30.0	133.6			African (m)	78
		30.0	130.5			African (f)	78
Average			**149.3**		**146.6 - 166.2**		
Adult (small)							
Mt I	D3442	4.74	**143.0**			Combined data	75

Supplementary Table S7. Estimation of encephalization quotient (EQ)

Individual	Estimated brain mass (g)	Estimated average body mass (kg)	EQ
subadult	560	41.2	2.96
		49.4[1]	2.57
large adult	632[2]	48.8	2.94
small adult	582	40.2	3.13

[1] estimated body mass at adulthood (120% of 41.2 kg)
[2] average of D2280, D2700, and D3444

S9. Character states identified in the Dmanisi postcranial remains

Table S8 summarizes states for characters identified on the Dmanisi postcranial remains and provides a tentative ordering of character states from primitive (dark shading) versus derived (light shading or white). The Dmanisi hominins exhibit an array of symplesiomorphic characters that group them with australopiths and earliest *Homo*, while KNM-WT15000 appears more derived in several features. KNM-WT15000 and Dmanisi share an array of synapomorphies with modern humans but are more primitive than modern humans in most features.

Supplementary Table S8. Character states of Dmanisi postcranial elements

	chimpanzees	australopiths	earliest *Homo*	Dmanisi	*H. erectus* (WT15000)	modern humans
Scapula						
orientation of glenoid cavity	cranial	cranial	-	cranial	cranial	lateral
l/w ratio of coracoid process	high	-	-	high	-	low
glenocoracoid angle	narrow	-	-	narrow	narrow	wide
b/l ratio of spine	low	-	-	high	high	high
Clavicle						
shaft length relative to humeral length	long	-	-	middle	middle	short
shape of conoid tubercle (relative a-p diameter)	small	-	large	large	large	large
Humerus						
position of lateral epicondyle rel. to lat. condyle	high	middle	middle	middle	-	low
degree of torsion	high	low	-	low	middle	high
Vertebrae						
canal shape (direction of greatest width)	dorsoventral	transversal	-	transversal	transversal	transversal
C2 spinal process	long	short	-	short	-	short
C2 sup. articular surface angle	narrow	narrow	-	narrow	-	wide
Th&L centrum area relative to body mass	small	middle	-	middle	middle	large
thoracic zygapophyseal joint angle	wide	middle	-	middle	wide	narrow
lumbar zygapophyseal joint angle	narrow	narrow	-	slightly wide	narrow	narrow
wedging of lumbar vertebrae	anterior	posterior	-	posterior	posterior	posterior
Femur						
elevation of greater trochanter	high	middle	middle	middle	-	low
bicondylar angle	wide	narrow	narrow	narrow	narrow	narrow
Tibia						
rel. size of joint surfaces	large	-	-	large	-	small
degree of torsion	high	-	-	low	-	low
Talus						
neck angle	wide	middle	middle	middle		narrow
flexor hallucis longus groove	deep, longitudinal	-	-	shallow, oblique	-	shallow, vertical
medial tubercles	2 prominent tubercles	-	-	2 prominent tubercles	-	prominent lateral tubercle
Metatarsals						
Mt1 torsion	wide	-	-	narrow	-	narrow
Mt I head size	small	large	large	large	-	large
Mt III, IV shaft torsion	narrow	-	wide	wide	-	wide
transversal and longitudinal pedal arching	absent	-	present	present	-	present
Body dimensions						
limb proportions (humerus/femur ratio)	high	middle	low	low	low	low
body mass	low	low	middle	middle	high	high
EQ	2.38	2.4 – 3.1	3.1	2.7 – 2.8	2.7 – 3.8	6.28

Supplementary References (continued from main text)

51. Fortelius, M., Werdelin, L., Andrews, P., Bernor, R. L., Gentry, A. *et al.* in *The Evolution of Western Eurasian Neogene Mammal Faunas* (eds. Bernor, R. L., Fahlbusch, V. & Mittmann, H.-W.) 414-448 (Columbia University Press, New York, 1996).
52. Simpson, C. G. Mammals and the nature of continents. *Am. J. Sci.* **241**, 1-31 (1943).
53. Sokal, R. R. & Sneath, P. H. A. *Principles of Numerical Taxonomy* (Freeman and Co, San Francisco, 1963).
54. Archer, A. W. & Maples, C. G. Monte Carlo simulation of selected binomial similarity coefficients: effect of number of variables. *Palaios* **2**, 609-617 (1987).
55. Maples, C. G. & Archer, A. W. Monte Carlo simulation of selected binomial similarity coefficients (2): effect of sparse data. *Palaios* **3**, 95-103 (1988).
56. Bernor, R. L. in *New Interpretations of Ape and Human Ancestry* (eds. Ciochon, R. L. & Corruccini, R.) 21-64 (Plenum Press, New York, 1983).
57. Flynn, L. Faunal provinces and the Simpson coefficient. *Contrib.Geology, Univ. Wyoming Spec.* **3**, 317-338 (1986).
58. Bernor, R. L. & Rook, L. in *Recent Advances on Multidisciplinary Research at Rudabánya, Late Miocene (MN9), Hungary: a Compendium* (eds. Bernor, R. L., Kordos, L. & Rook, L.) 21-25 (Palaeontographia Italica, Pisa, 2003).
59. Turner, A. e. a. in *African Biogeography, Climate Change and Human Evolution* (eds. Bromage, T. G. & Schrenk, F.) 369-399 (Oxford University Press, 1999).
60. Tappen, M., Lordkipanidze, D., Bukshianidze, M., Vekua, A. & Ferring, R. in *African Taphonomy: A Tribute to the Career of C.K. "Bob" Brain* (eds. Pickering, T. R., Schick, K. & Toth, N.) (Oxford University Press, Bloomington, Indiana,, 2006).
61. Behrensmeyer, A. K. Taphonomic and ecologic information from bone weathering. *Paleobiology* **2**, 150-162 (1978).
62. Brain, C. K. *The Hunters or the Hunted* (University of Chicago Press, Chicago, 1981).
63. Villa, P. & Mahieu, E. Breakage patterns of human long bones. *J. Hum. Evol.* **21**, 27-48 (1991).
64. Horwitz, L. & Smith, P. in *Proceedings of the 1993 Bone Modification Conference* (eds. Hannus, L., Rossum, L. & Winham, R.) 188-194 (Archeology Laboratory, Augustana College, Hot Springs, South Dakota, 1993).
65. Horwitz, L. K. & Smith, P. The effects of striped hyaena activity on human remains. *J. Archaeol. Sci.* **15**, 471 - 481 (1988).
66. Haglund, W. D. & Sorg, M. H. *Forensic Taphonomy: the Postmortem Fate of Human Remains* (CRC Press LLC, Boca Raton, 1996).
67. Pickering, T. Carnivore voiding: A taphonomic process with the potential for the deposition of forensic evidence. *J. Archaeol. Sci.* **46**, 401-411 (2001).
68. Scheuer, L., Black, S. & Christie, A. *Developmental Juvenile Osteology* (Academic Press, California, 2000).
69. Martin, R. *Lehrbuch der Anthropologie in systematischer Darstellung mit besonderer Berücksichtigung der anthropologischen Methoden* (Fischer, Stuttgart, 1957-1966).

70. Etter, H. F. L'omoplate des primates supérieurs, la relation entre sa forme et sa function. *Archives Suisses d'Anthropologie Générale (Genève)* **48**, 31-51 (1984).
71. Singer, K. P., Breidahl, P. D. & Day, R. E. Variations in zygapophyseal joint orientation and level of transition at the throracolumbar junction. *Surg. Radiol. Anat.* **10**, 291-295 (1988).
72. McHenry, H. M. & Berger, L. R. Body proportions of *Australopithecus afarensis* and *A. africanus* and the origin of the genus *Homo*. *J. Hum. Evol.* **35**, 1-22 (1998).
73. Trotter, M. & Gleser, G. C. Estimation of stature from long bones of American Whites and Negroes. *Am J Phys Anthropol* **10**, 463–514 (1952).
74. Duyar, I. & Pelin, C. Body height estimation based on tibia length in different stature groups. *Am. J. Phys. Anthropol.* **122**, 23-27 (2003).
75. Byers, S., Akoshima, K. & Curran, B. Determination of adult stature from metatarsal length. *Am. J. Phys. Anthropol.* **79**, 275-279 (1989).
76. Martin, R.D. Adaptation and body size in primates. *Z. Morphol. Anthropol.* **71**, 115-124 (1980).
77. Martin, R. D. Relative brain size and basal metabolic rate in terresrial vertebrates. *Nature* **293**, 57-60 (1981).
78. Lundy, J. K. & Feldesman, M. R. Revised equation for estimating living stature from the long bone of the South African Negro. *S. Afr. J. Sci.* **83**, 54-55 (1987).